

APPLICATION OF KEY PERFORMANCE INDICATORS FOR TRAJECTORY PREDICTION ACCURACY

Stéphane Mondoloni, CSSI Inc., Washington, DC

Abstract

Key Performance Indicators (KPI) for trajectory prediction accuracy were applied to flights operating with a meet-time function enabled during climb. Comparison to flights operating open-loop reveals that the meet-time function alters the correlation between typical prediction accuracy metrics. Despite this, the same two KPI measures can be linearly combined in both the open- and closed-loop case to estimate the complete set of metrics with good rank correlation. The performance of a conflict detection function was evaluated as a function of these KPI to determine if these are predictive of conflict detection performance. In both open- and closed-loop cases, improvements in KPI led to improvements in CD performance across the System Operating Characteristics (SOC) curves. Similar SOC curves were obtained in both cases when the average KPIs were set to the same level, indicating that the TP accuracy KPI are predictive of CD performance.

Introduction

The ICAO Global Air Traffic Management (ATM) Operational Concept [1] indicates that “a key tenet of the operational concept is performance orientation”. It is clear that future changes to the ATM system must be *performance-driven*, implying the need to both trace the performance impact of changes to the system, and the need to derive required performance on systems due to demands on service-delivery performance. Central to this goal lays the need to be able to express, in a compact manner, the performance of the interacting elements comprising the ATM system. One such element is a trajectory prediction (TP) system. This paper addresses the compact expression of TP performance and its relationship to dependent ATM automation.

At the heart of many future ATM automation systems is the trajectory predictor, delivering forecasts of aircraft trajectories upon which automation tools base advisories. The performance of the automation systems is a strong function of the quality of the prediction supplied by the TP. This TP quality has typically been expressed using metrics tailored to the specific automation system being evaluated ([2]-[9]). The result is a collection of investigations with TP performance expressed using a broad range of metrics. This makes it

difficult to determine the “state-of-the-art”, makes TP-performance impact analysis an ad-hoc process and impedes the sharing of TP capabilities across automation systems. In this area, effort is required to achieve the seamless, globally interoperable system called for in the ICAO Global ATM Operational Concept.

Looking forward to the Next Generation (NextGen) ATM System, this concept relies upon various capabilities such as trajectory based operations (TBO) and performance-based services [10]. Central to TBO is the four-dimensional trajectory (4DT), upon which certain tactical functions will act. Included in these are: Tactical Separation Management (TSM) and Tactical Trajectory Management (TTM). Both of these functions rely on trajectory prediction to determine when intervention is required, and to develop viable plans for intervening. As a result of this reliance, the performance of both TSM and TTM will be impacted by the performance of trajectory prediction. In the case of TSM, as TP accuracy degrades, so will TSM performance (e.g., as in [11]). The TTM function seeks to provide Controlled Times of Arrival (CTA) subject to minimizing conflict likelihoods. To this end, TP accuracy is required to determine likelihoods in a CTA environment. This study will investigate TP performance with time-control functionality.

Network-Enabled Operations allow trajectory prediction to migrate towards a common subscription service. For this purpose, the ability to receive TP quality measures in a harmonized manner allows applications to dynamically evaluate the impact of uncertainty. For example, an application receiving predicted trajectories can tailor output based upon the quality of the trajectory. Alternatively, applications may specify minimum requirements on prediction. All of the above is facilitated through the introduction of key performance indicators (KPI) on trajectory predictors. These reduce the performance of the TP to a standard small set of measures that can be applied for the above purposes.

Prediction Accuracy

Many prior efforts describe the trajectory prediction problem, the measurement of accuracy and associated input data concerns (e.g., [12]-[22]). The description of predicted trajectory accuracy is complicated by the fact that errors in prediction are a signal and not a simple

point measure. For example, as represented in Figure 1, the altitude error between a “truth” trajectory and forecast trajectory will not be a simple function of time. Further complexities include: the error signal will vary with time at which the forecast occurs, input data quality is critical to TP performance, and the specific conditions under which the TP is evaluated impact the performance.

Studies on TP accuracy have frequently focused on improving accuracy for the purposes of improving a specific application using TP. These have led to various point measurements being considered as representing TP performance. These point measures are typically time or spatially coincident [21], with cross-track, along-track and vertical errors at fixed look-ahead being frequently investigated (e.g., [4]-[8]). Time errors were also reported relative to flight events such as top-of-descent or crossing a specified fix. Despite the multi-dimensional aspect to trajectory prediction errors, we know [15] that output errors can be modeled through a linear, time-varying propagation of input errors and disturbances. What this implies is that many of the reported TP errors are correlated, and this fact can be exploited to derive a minimum set of key performance indicators [23], representative of overall TP accuracy.

This study investigates the application of TP accuracy KPI to trajectories subject to required time-of-arrival functionality. While a prior effort investigated open-loop trajectories, with the NexGen movement towards CTAs, the ability to apply these KPI to closed-loop trajectories is required and investigated herein. This study also demonstrates the application of these TP indicators to the performance evaluation of a dependent conflict detection function, as will be necessary as we move to the performance-based ICAO Global ATM operational concept.

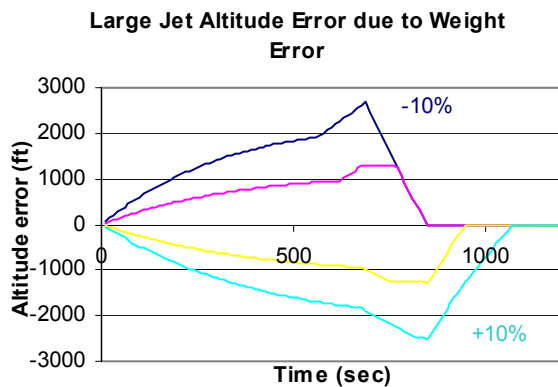


Figure 1 Example trajectory prediction accuracy signals

Method

This study addresses the application of TP accuracy key performance indicators (KPI). This effort determined the applicability of KPI for trajectories operating under differing control modes (e.g., a meet-time mode). The study then addresses the ability to apply the KPI for evaluation of DST performance such as a conflict probe.

The overall approach involved simulating a set of trajectories under various scenarios and subject to uncertainties. The comparison of a perfect forecast with an uncertain forecast provided a set of error metrics that were used to determine TP accuracy KPI. This was done for climbing flights with and without an RTA-meeting capability. The performance of a conflict detection algorithm using these trajectories was evaluated to determine if the TP KPI are predictive of CD performance. These steps are described in more detail below.

Scenarios

A set of scenarios was developed in order to investigate trajectory prediction performance under a set of conditions representative of current operations. To this end, the following steps were taken:

- Selected a random day without adverse weather effects (11/19/2004)
- Obtained flown flight information for all flights including path, profile, aircraft types, departure and arrival information. Preserved only those flights for which we had complete information and aircraft performance models.
- Obtained forecast winds aloft
- Found the CAS/Mach schedule and weight combination that best fit the observed climb profile. This was used to obtain distributions (by aircraft model) on the weight and speed schedules as input to a Monte Carlo simulation.
- Obtained parameters (Mach, CAS, weight) for each flight in the sample from the appropriate distribution and ensured that performance constraints were not violated.

The above resulted in a set of baseline conditions from which a set of baseline trajectories were generated using point-mass aircraft performance modeling. Each baseline trajectory represents the initial forecast trajectory.

Two “truth” trajectory scenarios were developed for each flight using either the same control targets (constant CAS/Mach climb) as above, or using the RTA algorithm described below. Truth trajectories incorporated the

effects of modeling errors and disturbances. These include errors in: weight, CAS target, Mach target and drag in addition to wind uncertainty. The range of allowable errors was limited to ensure that operating parameters were not exceeded for any flight. Wind uncertainty was modeled in accordance with the model described in [24] allowing for wind error autocorrelations (along-track and altitude) to be consistent with empirical data. When investigating airborne scenarios, smaller modeling errors were applied, in addition to zero errors in speed targets.

Derivation of Accuracy KPI

A prior effort [23] investigated the derivation of accuracy KPI for trajectory prediction with errors commensurate with ground-derived trajectories. This study investigates the applicability of these KPI to an airborne-derived trajectory under control to meet an RTA.

A collection of 16 TP accuracy measures was collected for each flight as follows:

- **Fixed look-ahead time** – Altitude error and along-track error at a look-ahead time of 600 and 900 seconds.
- **Fixed distance along-path** – Altitude and time errors at along-track distances of 25, 50 and 75 nautical miles
- **Fixed flight level** – Time and along-track errors upon crossing 20,000 and 30,000 feet (if applicable).
- **Derived measures** – Peak and average altitude (co-temporal) error over the duration of the climb

The above gives a set of 16 TP accuracy measures for each flight in a scenario. The objective is to reduce the set of 16 to a smaller set of *key* performance indicators that represent the behavior. To this end, we applied factor analysis to determine the dimensionality of the problem. For example, if analysis revealed a one-dimensional problem, all measures would lie on a line and a single KPI would be sufficient.

Briefly, factor analysis seeks to express the vector of metrics for each flight \mathbf{x} (with length 16) as a linear combination of an unknown, but reduced dimension vector \mathbf{y} as follows:

$$\vec{\mathbf{x}} = \vec{\mu} + \Gamma \vec{\mathbf{y}} + \vec{\mathbf{e}} \quad (1)$$

The vector \mathbf{e} is a residual vector with elements that are uncorrelated and normally distributed with zero mean. The error metrics are assumed to be normally distributed with the measured sample variance. Given the number of factors, maximum likelihood estimation is applied to

obtain the reduced dimension model in terms of the matrix Γ and the variance of \mathbf{e} .

The elements of the \mathbf{y} vector are taken to be the KPI. In practice, the elements of the \mathbf{y} vector will correspond to one of the 16 performance metrics as the Γ matrix will have several rows for which only one element contributes significantly.

A prior investigation revealed that a 2-factor model was sufficient when lateral-path deviations were not incorporated. In this case, the KPI were: peak altitude error and along-track error at 600 seconds. We use these as a starting point for this investigation. The result of the analysis indicates that the entire collection of metrics can be *estimated* by a linear combination of the KPI:

$$\langle \vec{\mathbf{x}} \rangle = \Lambda \begin{pmatrix} KPI_1 \\ KPI_2 \end{pmatrix} \quad (2)$$

While substantial variability will remain in some metrics, rank correlation is applied to determine whether the relative rank of the estimated measures correspond to the actual.

RTA Algorithm

Scenarios meeting a required time of arrival (RTA) were developed by applying an RTA-meeting algorithm similar to that described in [25]. To illustrate the process, we consider a climbing flight subject to an RTA at some downstream point along the flight path (see Figure 2). A nominal flight trajectory is first generated from an initial condition to beyond the desired RTA point. As the flight progresses, atmospheric disturbances and modeling errors perturb the trajectory away from the nominal path and affect the estimated time of arrival (ETA) at the RTA waypoint. For this reason, at fixed intervals along the flight, a new projected flight trajectory is computed and an ETA is obtained. If the error between the ETA and RTA exceeds a threshold defined by a control “funnel” as described in [25], the aircraft speed schedule is modified for the remainder of the climb and cruise segment.

Both the CAS and Mach targets are modified in proportion to the ratio of the time error (ETA – RTA) to the time-to-go. However, as errors may accumulate beyond the controllable range, limits on the speed targets are computed as follows:

- Target CAS and Mach must not exceed maximum operational values
- If the flight is below a new transition altitude, the new transition altitude must support a minimum 500 feet-per-minute climb rate at maximum climb power

- The speed schedule must allow a minimum 500 feet-per-minute climb at the top-of-climb point

If the new speed targets prevent the above, the targets are adjusted until the constraints can all be met. One likely outcome to hitting these speed constraints is that the RTA will not be met.

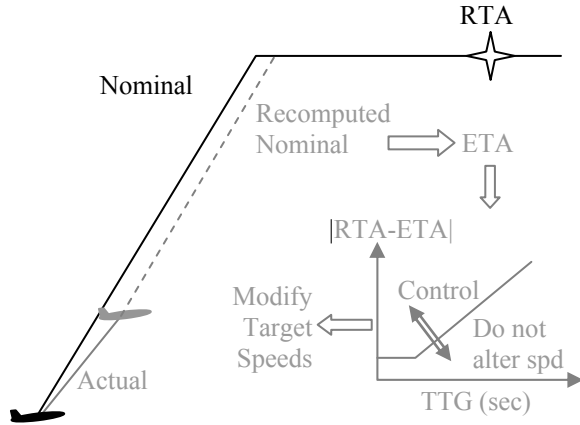


Figure 2 Illustration of RTA Algorithm

In addition to limiting the speeds as above, speed targets are not instantaneously met. Acceleration (or deceleration) segments are required and limits are prescribed to allow the flight to continue climbing during these segments.

Method for Conflict Probe Assessment

One of the objectives for development of TP accuracy KPI was to be able to assess the effect of TP performance on DST performance via the TP performance KPI. This is illustrated starting with a basic application of TP, a conflict detection tool.

Conflict detection performance is typically (e.g., [26]) described through “system operating characteristic” (SOC) curves illustrating the tradeoff between false alerts (detected conflicts that do not materialize) and missed alerts (conflicts that happen but go undetected). In this work, false and missed alert rates are defined as follows.

$$FA = \frac{N_F}{(N_T + N_F + N_M)} \quad (3)$$

$$MA = \frac{N_M}{(N_T + N_F + N_M)}$$

The rates are normalized by the sum of the number of true (T), false (F) and missed (M) alerts to ensure a range [0, 1]. The SOC are derived by allowing the separation used for detection to increase beyond the separation standard. As this buffer is increased, CD misses fewer

conflicts and captures more missed alerts. The tradeoff is illustrated in Figure 3.

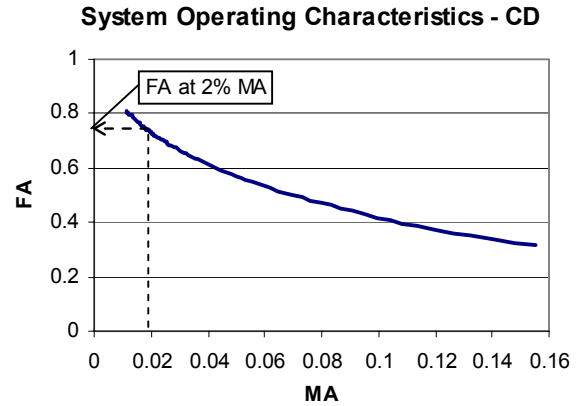


Figure 3 Example of SOC for CD

These rates (MA and FA) are obtained by running a CD algorithm on both the truth and forecast scenario with a buffer applied to separation in the forecast scenario. A pairwise comparison of conflicts between scenarios is used to determine whether a conflict is true, false or missed.

For evaluation of KPI, the SOC are derived for all flights with KPI below a threshold value. For example, for the along-track error at 10 minutes KPI (dx_600), SOC curves would be derived from conflicts pertaining to aircraft with this KPI below a threshold (e.g. 10,000 feet). This is repeated by varying the threshold for each KPI individually.

Once the SOC have been derived, the tradeoff between various KPI is complicated by the number of degrees-of-freedom. For the purposes of evaluating these trades, we can reduce the SOC curve to a single number by assuming that an acceptable level of missed alerts would be specified. The resulting false alert rate at that MA value would indicate the overall performance (see Figure 3). For this study, an “acceptable” MA of 2% was selected, representing a low value of missed alerts.

Results

This section evaluates the RTA functionality described previously and compares the relationship between TP accuracy metrics to flights without time control. The application of TP KPI for conflict detection performance evaluation is presented.

Evaluation of RTA Functionality

The RTA functionality was evaluated in a simulation and compared to an open-loop scenario assuming the same modeling errors and atmospheric disturbances. In this case, the RTA point was at a 15

minute look-ahead point in the baseline. The error in time-of-arrival at the RTA point was reduced from an RMS of 18.1 seconds in the open-loop to an RMS error of 6.8 seconds in the controlled case. For this example, a tolerance of 5 seconds on meeting RTA was employed. A histogram of the change in error is shown in Figure 4. Not all time errors can be successfully controlled due to the limits in speed as described previously.

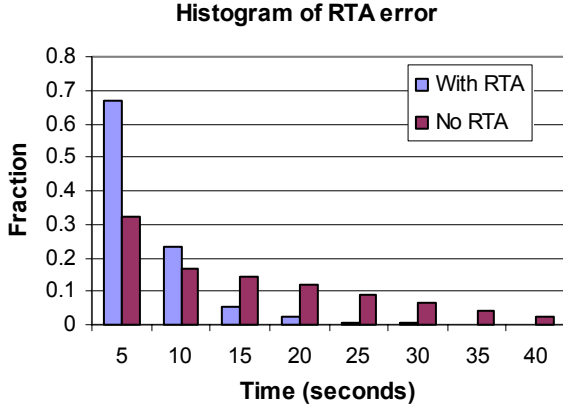


Figure 4 Histogram of time-of-arrival error

While the time-of-arrival estimate at the RTA point was improved, other metrics had increases and decreases in RMS error. This can be understood by realizing that the RTA was achieved during climb by trading off altitude accuracy to achieve greater along-track and temporal accuracy. For example, the RMS in peak altitude error increased from 804 feet to 986 feet in the above scenario, whereas the along-track RMS error at 900 seconds decreased from 12700 to 4900 feet. These results are consistent with estimates, as the along-track RMS error reduction would be proportional to the reduction in time error. The altitude error requires some explanation.

Control to reduce the time of arrival error will lead to a change in speed. The speed change will impact the climb rate through the following relation:

$$\frac{dh}{dt} = \frac{\left(\frac{T-D}{mg}\right)}{\left[\frac{1}{g} \frac{dV}{dh} + \frac{1}{g} \frac{dw}{dh} + \frac{1}{V}\right]} \quad (4)$$

$$\frac{d}{dV} \left(\frac{dh}{dt} \right) \approx \frac{-2/V}{\frac{dV}{dh} + 1} + \frac{\left(\frac{T-D}{mg}\right)}{\left(\frac{dV}{dh} + 1\right)^2}$$

The approximation of zero wind (w) is made in the second equation. Typically the first term dominates and an increase in speed leads to a decrease in climb rate. Since the altitude error is uncorrelated with the time-of-arrival (TOA) error in the open-loop case (see [23]), the reduction in variance of TOA error, through a speed change in the closed-loop case, increases variance of the altitude error. Substituting typical values for the parameters allows one to crudely estimate that the 11 second reduction in TOA error results in roughly a 200 foot increase in the RMS of peak altitude error (versus an observed 182 foot difference).

Comparing the relationship between metrics in the open-loop (Table 1) versus the RTA-meeting case (Table 2) indicates that the closed-loop case alters the correlation between metrics. In particular, the time error at distance and the distance error at time metrics were largely uncorrelated from altitude errors in the open-loop case. By closing the loop, a correlation is introduced.

In a perfectly controlled case, the time error would be small in the closed loop case. However, the system is not perfectly controlled, primarily due to flights operating near speed limits subject to larger errors. Two situations can develop:

- **A late flight** – The flight misses the RTA since it cannot increase speed further. The increase in speed results in the actual climb rate being below the forecast.
- **An early flight** – The flight misses the RTA since it cannot reduce the speed further. The reduction in speed results in the actual climb rate being above the forecast.

The above behaviors are observed for flights with large TOA errors and explain how the closed loop control introduces correlation not present in the open-loop case.

The loss of correlation with altitude at fixed distance is more complex. The reason for the change in speed to meet a TOA stems from an early or late arrival at a point. In a climb, an early flight would have been below the predicted altitude at a fixed distance. The corresponding decrease in speed to meet the RTA would lead to a competing increase in altitude. The result is dependent on circumstance and leads to a zero correlation in a diverse sample.

Table 1 Correlation coefficients between metrics – open-loop

	Peak Altitude	Average Altitude	dh at 600 secs	dh at 50NMI	dx at 600 secs	dx at FL200	dt at 50NM	dt at FL200
Peak_alt	1.00	0.98	0.87	0.84	0.00	-0.73	-0.05	-0.85
avg_alt	0.98	1.00	0.88	0.87	-0.01	-0.78	-0.03	-0.89
dh_600	0.87	0.88	1.00	0.79	0.00	-0.66	-0.05	-0.76
dh_50NMI	0.84	0.87	0.79	1.00	-0.37	-0.81	0.32	-0.79
dx_600	0.00	-0.01	0.00	-0.37	1.00	0.36	-0.97	0.03
dx_FL200	-0.73	-0.78	-0.66	-0.81	0.36	1.00	-0.37	0.92
dt_50NM	-0.05	-0.03	-0.05	0.32	-0.97	-0.37	1.00	-0.02
dt_FL200	-0.85	-0.89	-0.76	-0.79	0.03	0.92	-0.02	1.00

Table 2 Correlation coefficients between metrics - with RTA

	Peak Altitude	Average Altitude	dh at 600 secs	dh at 50NMI	dx at 600 secs	dx at FL200	dt at 50NM	dt at FL200
Peak_alt	1.00	0.95	0.87	0.62	0.58	-0.40	-0.57	-0.65
avg_alt	0.95	1.00	0.95	0.78	0.49	-0.57	-0.49	-0.79
dh_600	0.87	0.95	1.00	0.79	0.46	-0.52	-0.49	-0.75
dh_50NMI	0.62	0.78	0.79	1.00	-0.03	-0.77	-0.01	-0.83
dx_600	0.58	0.49	0.46	-0.03	1.00	0.24	-0.96	-0.14
dx_FL200	-0.40	-0.57	-0.52	-0.77	0.24	1.00	-0.27	0.90
dt_50NM	-0.57	-0.49	-0.49	-0.01	-0.96	-0.27	1.00	0.13
dt_FL200	-0.65	-0.79	-0.75	-0.83	-0.14	0.90	0.13	1.00

The correlations indicate greater coupling between dimensions for the case with the RTA. However, when comparing the open and closed loop cases, a factor analysis with two factors reveals the same dominant terms in each load vector. Practically what this implies is that the Λ matrix (see equation 2) will have stronger off-diagonal terms when fit to the RTA-meeting case.

A comparison of the rank correlation (using Spearman ρ) between the estimated metrics and the measured metrics was conducted for two cases. One case used the Λ matrix from the open-loop case to estimate the closed-loop data using the closed-loop KPI values. The second case used a Λ matrix derived from the closed-loop data. For this example, we used the better-fitting average altitude error and along-track error at 600 feet as the KPI. This is in contrast to [23] which looked at the peak altitude error. Table 3 shows these results.

The rank correlation across all metrics improves *slightly* when the fitting matrix (Λ) is conditioned on the nature of the aircraft control systems. Overall, the degree of correlation is good and indicates that the KPI should be predictive of TP performance as expressed by the collection of metrics.

Table 3 Rank Correlation Comparison

Metrics	Spearman ρ	
	$\Lambda_{open-loop}$	$\Lambda_{closed-loop}$
Peak altitude	.94	.95
Δh at 600 secs	.95	.95
Δh at 900 secs	.89	.90
Δh at 25NMI	.74	.85
Δh at 50NMI	.89	.91
Δh at 75NMI	.93	.94
Δx at 900 secs	.79	.79
Δx at FL200	.74	.83
Δx at FL300	.86	.85
Δt at 25NMI	.87	.87
Δt at 50NMI	.97	.97
Δt at 75NMI	.97	.97
Δt at FL200	.81	.85
Δt at FL300	.89	.89

Use of KPI for Conflict Probe Evaluation

System Operating Characteristics for a conflict detection function were derived for the open-loop case. The variation of the performance with each threshold KPI (applied independently) is shown in Figure 5 for along-track and Figure 6 for altitude. The figures show that improvement in CD performance occurs as each KPI is improved independently.

CD performance with RTA functionality enabled is illustrated in Figure 7 and Figure 8. The case with unconstrained KPI (labeled "ALL") is improved from the open-loop case through the addition of the meet-time function. This is consistent with the KPI being indicative of TP performance, as the *RMS* along-track KPI is reduced from 8311 to 5412 feet with the introduction of the RTA function.

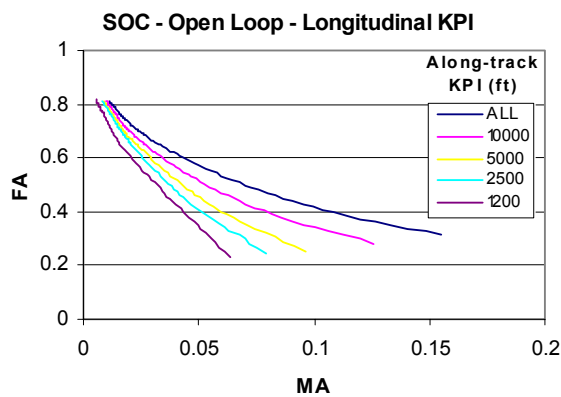


Figure 5 SOC variation with Longitudinal KPI (open-loop case)

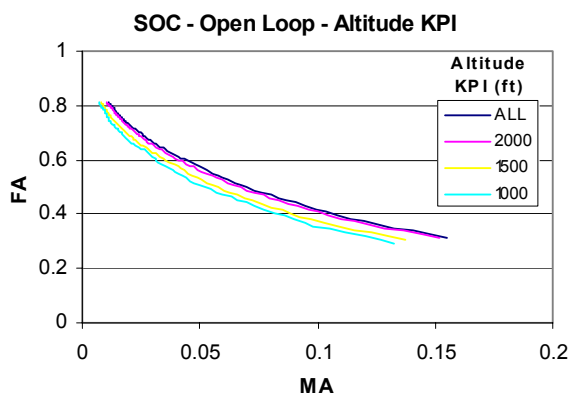


Figure 6 SOC variation with Altitude KPI (open-loop case)

The curves in Figure 5 through Figure 8 illustrate the effect of KPI by applying a threshold on the KPI (i.e., $KPI < \text{threshold}$). However, the distribution of KPI for the set of flights is likely to impact CD performance. Supporting evidence is obtained by deriving the SOC for

the open-loop versus closed-loop case when the RMS values of both KPI are close to each other (Figure 9). While the curves are close to each other, the closed-loop case performs better at high MA rates whereas the open-loop case performs better at lower MA rates. This is due to the different distribution of KPI in each case. Recall that the closed-loop case reduces the variance in the KPI across the data set. Given the same RMS, the reduced variance in the closed-loop case requires a broader range of KPI. At small buffer sizes, the closed-loop case will have captured more conflict pairs with small errors, leading to a low MA rate. At large buffer sizes, the missed alerts will be due to the greater fraction of larger errors in the closed-loop case.

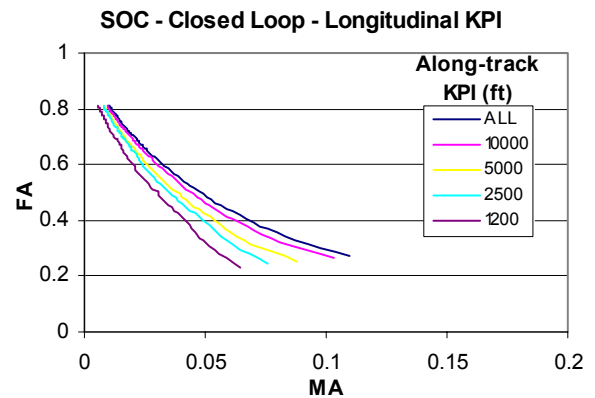


Figure 7 SOC Variation with Longitudinal KPI (closed-loop case)

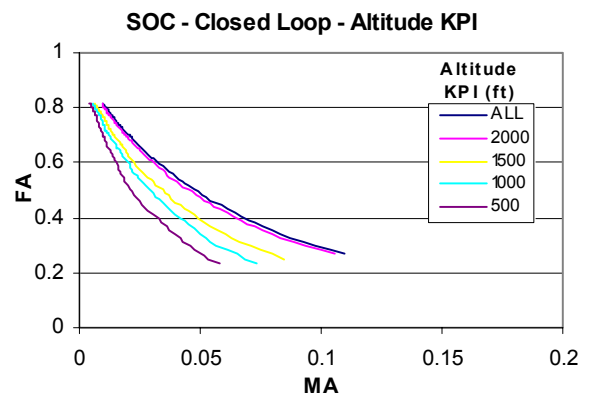


Figure 8 SOC Variation with Altitude KPI (closed-loop case)

The tradeoff between the along-track and altitude KPI was investigated in both cases by looking at the FA rate at a MA rate of 2%. Contour plots of this FA rate are presented against the threshold KPI values in Figure 10 and Figure 11. As each KPI is reduced independently, the FA rate typically decreases. The coupling between KPIs introduced in the closed loop

case explains the “flattening” of the contours for low threshold values of the KPI. For example, when altitude errors are low, along-track errors will also be low, leading to limited variation in performance as the along-track KPI threshold is lowered.

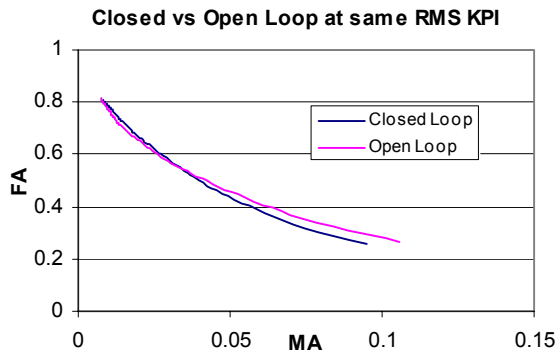


Figure 9 Comparison open vs closed-loop at same RMS KPI values

As we showed earlier, the specific control-law investigated allows a tradeoff of one KPI for the other. This trade can be represented as a curve on the contour plot. By determining the point on the curve providing the minimum FA rate, an optimum operating point can be determined. This may be a useful consideration (not the only factor) when specifying levels of tolerance for RTA being applied for other purposes, such as flow control. For example, specifying too tight a tolerance would drive down one KPI at the expense of another, potentially worsening the performance of detection.

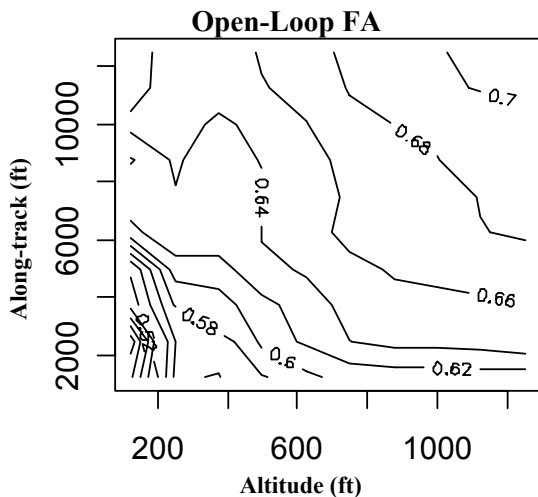


Figure 10 FA rate at fixed 2% MA rate KPI trade space (open loop case)

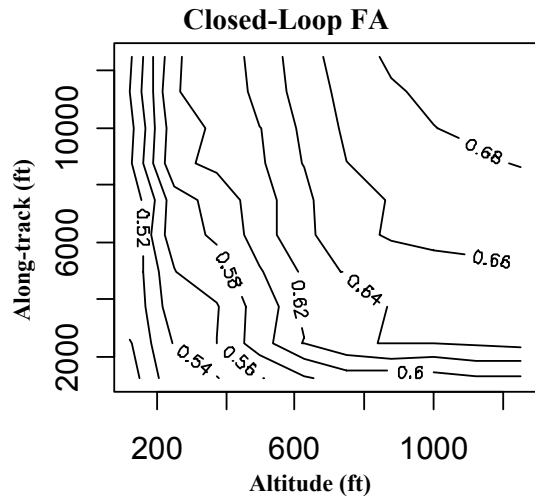


Figure 11 FA rate at fixed 2% MA rate KPI trade space (closed loop case)

Conclusions

This effort applied key performance indicators for trajectory prediction accuracy to flights operating with a meet-time function enabled. While the introduction of this control resulted in a correlation between previously independent TP accuracy metrics, a linear combination of the KPI could provide estimates of metrics with good rank correlation. This correlation improved slightly when the fitting matrix was conditioned on the type of control. Error sources in this study were selected to be representative of airborne trajectory prediction.

Conflict detection performance was improved with a reduction in either KPI as illustrated by SOC curves for conflict detection. The introduction of time-of-arrival control resulted in a shift in the distribution of KPI across all flights in the sample towards lower along-track errors. This resulted in a beneficial shift of the SOC curves at any combination of *threshold* KPI. However, the SOC curves were more closely aligned when the average along-track error and altitude error matched between the cases. Some discrepancies were still found due to the differences in distribution within the samples. Further investigations could generate samples with identical KPI for all flights in the sample.

The application of time control using the described algorithm resulted in along-track error being traded for altitude uncertainty. For control with this type of trade, an operating point can be derived by optimizing conflict detection performance given a specified maximum missed alert rate. While the trade space indicates the most CD-favorable direction to improve TP

performance, not all directions may be possible as changes to one KPI may lead to changes in the other.

This study investigated only two of the three KPI dimensions necessary to describe TP accuracy. The third term, due to errors in path, was not considered here but is likely to also be coupled with other errors. This error may reduce in importance in the future as RNP levels seek to define paths to increasing levels of precision.

The issue of confidence in TP accuracy was not addressed. For open-loop trajectories, if this can be established in the modeling errors, the issue becomes one of confidence in the accuracy of the input data to the predictor. For closed-loop trajectories, one must also establish confidence in the ability to control for disturbances and errors.

Going forward, key performance indicators on trajectory prediction accuracy can suit a variety of purposes, including:

- Uniform reporting of TP accuracy in the technical literature
- Specification of TP requirements by DST developers
- Quality measure for a trajectory distributed to multiple applications in a networked environment
- Minimum performance standard for a down-linked trajectory requesting an ATM service-delivery level.

Acknowledgement

This study was conducted as part of FAA/EUROCONTROL Action-Plan 16 activities. Action Plan 16 is entitled “Common Trajectory Prediction Capabilities”.

References

[1] International Civil Aviation Organization (ICAO), 2005, “Global Air Traffic Management Operational Concept”, Doc 9854 AN/458, First Edition

[2] Erzberger, H., R.A. Paeilli, D.R. Isaacson, M.M. Eshowl, 1997, “Conflict Detection in the Presence of Prediction Error”, FAA / Eurocontrol ATM R&D Seminar, Saclay, FR

[3] Swierstra, S., S. Green, 2003, “Common Trajectory Prediction Capability for Decision Support Tools”, 5th USA/Eurocontrol ATM R&D Seminar, Budapest, Hungary

[4] Wanke, C., 1997, “Using Air-Ground Data Link to Improve Air Traffic Management Decision Support

System Performance”, FAA/Eurocontrol ATM R&D Seminar, Saclay, FR

[5] Green, S.M., M.P. Grace, D.H. Williams, 2000, “Flight Test Results: CTAS and FMS Cruise/Descent Trajectory Prediction Accuracy”, 3rd FAA Eurocontrol ATM R&D Seminar, Naples, IT

[6] Williams, D.H., S.M. Green, 1998, “Flight Evaluation of Center-TRACON Automation System Trajectory Prediction Process”, NASA/TP-1998-208439

[7] Green, S., R. Vivona, 1996, Field Evaluation of Descent Advisor Trajectory Prediction Accuracy. AIAA GN&C Conference, San Diego, CA

[8] Mueller, K.T., et al, 2002, “Strategic Aircraft Trajectory Prediction Uncertainty and Statistical Sector Traffic Load Modeling”, AIAA-2002-4765 AIAA GN&C Conference, Monterey, CA

[9] Coppenbarger, R., R. Lanier, D. Sweet, S. Dorsky, 2004, “Design and Development of the En Route Descent Advisor (EDA) for Conflict-Free Arrival Metering”, AIAA-2004-4875, AIAA GN&C Conference, Providence, RI.

[10] Joint Planning and Development Office (JPDO), 2006, Concept of Operations for the Next Generation Air Transportation System – DRAFT

[11] Arthur, W. C., M.P. McLaughlin, 1998, “User Request Evaluation Tool (URET) Interfacility Conflict Probe Performance Assessment”, 2nd USA/Europe ATM R&D Seminar, Orlando, FL

[12] Mondoloni, S., I. Bayraktutar, 2005, “Impact of Factors, Conditions and Metrics on Trajectory Prediction Accuracy”, 6th USA/Europe ATM R&D Seminar, Baltimore, MD

[13] Jackson, M. R., J.Z. Yiyuan, R.A. Slattery, 1999, “Sensitivity of Trajectory Prediction in Air Traffic Management”, Journal of Guidance, Control and Dynamics, Vol. 22 No. 2

[14] Jackson, M.R., Y. Zhao, R. Slattery, 1996, “Effects of Modeling Errors on Trajectory Prediction in Air Traffic Control Automation”, AIAA-96-3721, AIAA GN&C Conference, San Diego, CA

[15] Waanders, T.C., 2005, “Propagation of Trajectory Prediction Uncertainties in the Vertical Plane”, Masters Thesis, Delft University of Technology, NL

[16] Hunter, G., 2004, “Towards a Standardized Reference Set of Trajectory Modeling Errors”, AIAA 2004-5037, AIAA Modeling and Simulation Technologies Conference, Providence, RI

- [17] Slattery, R., Y. Zhao, 1997, "Trajectory Synthesis for Air Traffic Automation", *Journal of Guidance, Control and Dynamics*, Vol. 20, No. 2.
- [18] Paglione, M., M. L. Cale, H.F. Ryan, 1999, "Generic Metrics for the Estimation of the Prediction Accuracy of Aircraft to Aircraft Conflicts by a Strategic Conflict Probe Tool", *Air Traffic Control Quarterly*, Vol. 7, No. 3, pp. 147-165
- [19] Mondoloni, S., S. Swierstra, M. Paglione, 2005, "Assessing Trajectory Prediction Performance – Metrics Definition", 24th Digital Avionics Systems Conference, Washington, DC
- [20] Cole, R.E., S.M. Green, M. Jardin, B.E. Schwartz, S.G. Benjamin, 2000, "Wind Prediction Accuracy for Air Traffic Management Decision Support Tools", 3rd USA/Europe ATM R&D Seminar, Naples, IT
- [21] Ryan, H.F., M. Paglione, S.M. Green, 2004, "Review of Trajectory Accuracy Methodology and Comparison of Error Measurement Metrics", AIAA-2004-4787, AIAA Conference, Providence, RI
- [22] Mondoloni, S., M. Paglione, S. Green, 2002, "Trajectory Modeling Accuracy for Air Traffic Management Decision Support Tools", ICAS 2002 Congress, Toronto, ON
- [23] Mondoloni, S., 2006, "Development of Key Performance Indicators for Trajectory Prediction Accuracy", 25th Digital Avionics System Conference, Portland, OR
- [24] Mondoloni, S., 2006, "A multiple-scale model of wind prediction uncertainty and application to trajectory prediction", AIAA ATIO Conference, Wichita, KS
- [25] Wichman, K.D., G. Carlsson, L.G.V. Lindberg, August 2002, "Flight Trials: Runway-to-Runway Required Time of Arrival Evaluations for Time-Based ATM Environment – Final Results", AIAA-2002-4859, AIAA GN&C Conferences, Monterey, CA
- [26] Yang, L.C., J.K. Kuchar, 1998, "Using Intent Information in Probabilistic Conflict Analysis", AIAA-98-4237, AIAA GN&C Conference, Montreal, PQ

Biographies

Stéphane Mondoloni is Chief Scientist for CSSI Inc. where he leads CSSI's Research & Engineering ATM laboratory. For over 10 years, he has conducted research and analysis in Air Traffic Management for both the FAA and NASA. Dr. Mondoloni developed CSSI's OPGEN, a tool for aircraft trajectory optimization, and developed a prototype intent-based airborne conflict resolution function for NASA Langley Research Center. He has investigated the impact of uncertainty on aircraft trajectory prediction and is a contributor to the joint FAA/Eurocontrol Action Plan 16. Recent investigations have included: the development of approaches for investigating benefits of in-trail procedures in Oceanic airspace, the application of decision-analysis methods for investigating investment decisions and strategic planning for air carriers, the development of information needs within the flight object to support interoperability, and contributing to the development of performance-assessment methods for the ATM System. Dr. Mondoloni holds a B.S., M.S. and Ph.D. from the Massachusetts Institute of Technology all in Aeronautical engineering.